Article

Cross-Correlated Relaxation Enhanced H–C NMR Spectroscopy of Methyl Groups in Very High Molecular Weight Proteins and Protein Complexes

Vitali Tugarinov, Peter M. Hwang, Jason E. Ollerenshaw, and Lewis E. Kay

J. Am. Chem. Soc., **2003**, 125 (34), 10420-10428• DOI: 10.1021/ja030153x • Publication Date (Web): 05 August 2003

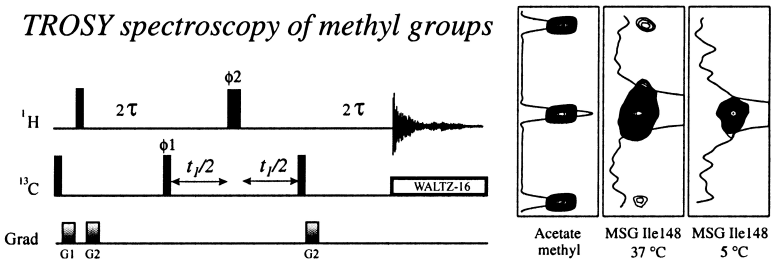

More About This Article

Additional resources and features associated with this article are available within the HTML version:

- Supporting Information
- Links to the 23 articles that cite this article, as of the time of this article download
- Access to high resolution figures
- Links to articles and content related to this article
- Copyright permission to reproduce figures and/or text from this article

View the Full Text HTML

Journal of the American Chemical Society is published by the American Chemical Society. 1155 Sixteenth Street N.W., Washington, DC 20036

J|A|C|S
ARTICLES
Published on Web 08/05/2003

Cross-Correlated Relaxation Enhanced $^{1}H-^{13}C$ NMR Spectroscopy of Methyl Groups in Very High Molecular Weight Proteins and Protein Complexes

Vitali Tugarinov, Peter M. Hwang, Jason E. Ollerenshaw, and Lewis E. Kay*

Contribution from the Protein Engineering Network Centers of Excellence and Departments of Medical Genetics, Biochemistry and Chemistry, The University of Toronto, Toronto, Ontario, Canada M5S 1A8

Received March 6, 2003; Revised Manuscript Received May 23, 2003; E-mail: kay@pound.med.utoronto.ca

Abstract: A comparison of HSQC and HMQC pulse schemes for recording $^{1}H-^{13}C$ correlation maps of protonated methyl groups in highly deuterated proteins is presented. It is shown that HMQC correlation maps can be as much as a factor of 3 more sensitive than their HSQC counterparts and that the sensitivity gains result from a TROSY effect that involves cancellation of intra-methyl dipolar relaxation interactions. $^{1}H-^{13}C$ correlation spectra are recorded on U-[^{15}N,^{2}H], Ileδ1-[^{13}C,^{1}H] samples of (i) malate synthase G, a 723 residue protein, at 37 and 5 °C, and of (ii) the protease ClpP, comprising 14 identical subunits, each with 193 residues (305 kDa), at 5 °C. The high quality of HMQC spectra obtained in short measuring times strongly suggests that methyl groups will be useful probes of structure and dynamics in supramolecular complexes.

Introduction

In the past several decades, solution NMR spectroscopy has evolved into an extremely powerful tool for the study of molecular structure and dynamics.[1,2] A major reason for the rapid maturation of the technique stems from the fact that the theoretical basis underlying complex multipulse experiments is well established[2]. It is therefore possible to calculate the response of a spin system to a particular pulse sequence and to design sophisticated schemes to manipulate spin−spin interactions in ways that allow extraction of the desired chemical information. A case in point has been the evolution of the field of protein NMR spectroscopy.[3,4] The development of multidimensional, multinuclear NMR experiments has been relatively straightforward because the underlying physics can be well explained by the equations of the density matrix and by simple pictures of how the bulk magnetization evolves in response to certain trains of pulses and delays. This has greatly simplified the description of NMR experiments and made an understanding of them accessible to a large subset of the NMR community.

Many of the NMR experiments that establish correlations between interacting spins on the basis of scalar coupled evolution can be well understood without considering the effects of relaxation directly.[5] For example, a qualitative description of the flow of magnetization in a triple resonance experiment, such as in a standard HNCO, can be given with focus only on the coherent transfer of magnetization between spins. On the other hand, certain classes of experiments, such as those that employ the TROSY principle,[6] are based on understanding the relaxation properties of each component of magnetization along the "pulse sequence trajectory", and in these cases, relaxation must be considered at each step in the experiment. In the case of TROSY spectroscopy, pulse schemes are designed whereby the longest-lived coherences are selected for and isolated from those that relax more efficiently. In many cases, very significant gains in sensitivity can be achieved with TROSY-based experiments.[7,8] A remarkable example from Wüthrich and co-workers involves the study of a 900 KDa GroEL−GroES complex in which an $^{1}HN-^{15}N$ correlation map of ^{15}N-labeled GroES in the complex was recorded.[9] Changes in the positions of $^{1}HN-^{15}N$ correlations between the free and bound forms of GroES were obtained for some residues, the first step in characterizing differences in structure and dynamics between free and bound states of this protein.

TROSY studies to date have made use of cross-correlation between dipolar and chemical shift anisotropy (CSA) relaxation mechanisms, focusing primarily on backbone amides[6] and on side chain aromatic groups.[10] We wish to examine here whether the methodology can be extended to applications involving side chain methyl groups. Our choice of methyls reflects the fact

(1) Wüthrich, K. *NMR of Proteins and Nucleic Acids*; John Wiley & Sons: New York, 1986.
(2) Ernst, R. R.; Bodenhausen, G.; Wokaun, A. *Principles of Nuclear Magnetic Resonance in One and Two Dimensions*; Oxford University Press: Oxford, 1987.
(3) Clore, G. M.; Gronenborn, A. M. *Science* **1991**, *252*, 1309.
(4) Bax, A. *Curr. Opin. Struct. Biol.* **1994**, *4*, 738−744.
(5) Kay, L. E.; Ikura, M.; Tschudin, R.; Bax, A. *J. Magn. Reson.* **1990**, *89*, 496−514.
(6) Pervushin, K.; Riek, R.; Wider, G.; Wüthrich, K. *Proc. Natl. Acad. Sci. U.S.A.* **1997**, *94*, 12366−12371.
(7) Salzmann, M.; Pervushin, K.; Wider, G.; Senn, H.; Wüthrich, K. *Proc. Natl. Acad. Sci. U.S.A.* **1998**, *95*, 13585−13590.
(8) Yang, D.; Kay, L. E. *J. Biomol. NMR* **1999**, *13*, 3−10.
(9) Fiaux, J.; Bertelsen, E. B.; Horwich, A. L.; Wuthrich, K. *Nature* **2002**, *418*, 207−221.
(10) Pervushin, K.; Riek, R.; Wider, G.; Wüthrich, K. *J. Am. Chem. Soc.* **1998**, *120*, 6394−6400.

10.1021/ja030153x CCC: $25.00

that (i) they are excellent probes of structure[11−13] and dynamics,[14,15] (ii) they give rise to well resolved spectra with good sensitivity,[16,17] (iii) they are dispersed throughout the primary structures of proteins and localized to the hydrophobic core, so that methyl−methyl distances obtained from NOE experiments provide a rich source of structural information,[11] and (iv) they are relaxed via an extensive network of cross-correlated interactions[18−21] that might be exploited for spectral sensitivity gains. Additionally, robust methods have been developed for obtaining highly deuterated ^{15}N, ^{13}C-labeled samples, with protonation exclusively at the methyl positions of Val, Leu, and Ile ($C^{\delta 1}$ only).[17] In cases where very dilute levels of protonation are required (see below), samples can also be prepared with protonation restricted to the Ile $C^{\delta 1}$ groups.[16]

Herein we examine a number of different approaches for recording ^{1}H−^{13}C correlation maps of methyl groups in highly deuterated, very high molecular weight proteins and protein complexes. Specifically, we show that it is possible to record ^{1}H−^{13}C TROSY-based correlation spectra of methyl groups in proteins in which substantial enhancement results from cancellation of intra-methyl ^{1}H−^{1}H and ^{1}H−^{13}C dipole−dipole relaxation interactions. Because of significant differences in the relaxation properties of the coherences that ultimately give rise to the signal observed in spectra of methyls, a description of the efficacy of correlation experiments must include the effects of relaxation at each step of the pulse sequence. The analysis for methyl groups is significantly more complex than what is required for AX spin systems in standard ^{1}HN−^{15}N TROSY experiments since there are 10 ^{1}H transitions and 8 ^{13}C transitions that must be taken into account in the case of a $^{13}C^1H_3$ spin system. Nevertheless, density matrix calculations can be easily employed in this situation, and the results of such calculations are summarized for the simple HMQC[22,23] and HSQC[24] pulse schemes that are examined here. Remarkably, the calculations show that the standard HMQC pulse sequence is optimized for TROSY spectroscopy "as is".

^{1}H−^{13}C correlation spectra of U-[^{15}N,^{2}H], Ileδ1-[^{13}C,^{1}H] malate synthase G (MSG), an 81.4 kDa single polypeptide enzyme comprised of 723 residues,[25] are presented at temperatures of 37 °C (45 ns correlation time) and 5 °C (approximately 118 ns correlation time). Spectra recorded at 5 °C on a U-[^{15}N,^{2}H], Ileδ1-[^{13}C,^{1}H] sample of the protease ClpP (a 14-mer with each subunit consisting of 193 amino acids for a total molecular weight of 305 kDa)[26] are also shown, illustrating that high sensitivity spectra of large complexes can be recorded in short measuring times. Remarkably, for a dilute concentration of protonated methyl groups in a protein, as is the case for the labeled systems mentioned above, HMQC-type experiments can be as much as a factor of 3 more sensitive than their HSQC counterparts. An explanation readily emerges from a detailed analysis of the HSQC/HMQC experiments and is presented here.

Materials and Methods

NMR Sample Preparation. A U-[^{15}N,^{2}H], Ileδ1-[^{13}C,^{1}H] sample of MSG was obtained by protein overexpression from a culture of *E. coli* BL21(DE3)pLysS cells in 1 L of D_2O M9 media as described in detail previously[27] using U-[^{2}H]-glucose (CIL, Andover, MA) and $^{15}NH_4Cl$ (CIL, Andover, MS) as the carbon and nitrogen sources, respectively, with the addition of 100 mg of 4-[^{13}C,^{1}H]-3,3-^{2}*H*-α-ketobutyrate to the growth medium 1 h prior to induction.[16] The sodium salt of 4-[^{13}C,^{1}H]-3,3-^{1}*H*-α-ketobutyric acid was obtained from Isotec (Miamisburg, OH), and the 3,3-[^{1}H] positions were exchanged to ^{2}H by incubation of a 2.7 mM solution of α-ketobutyrate, 99.9% D_2O, 45 °C at pH = 10.5 (uncorrected) for 20 h, following the procedure of Gardner et al.[16] MSG was purified as described earlier.[27] The NMR sample was 0.8 mM in protein [300 μL Shigemi cell (Shigemi Inc., US)] and contained 99.9% D_2O, 25 mM sodium phosphate, pH 7.1 (uncorrected), 20 mM $MgCl_2$, 0.05% NaN_3, 0.1 mg/mL Pefabloc, and 5 mM DTT. The use of U-[^{2}H]-glucose and 4-[^{13}C,^{1}H]-3,3-^{2}*H*-α-ketobutyrate as the sole carbon sources during protein production along with D_2O as the solvent in the NMR sample minimized protonation of all protein sites except for δ1 methyls of Ile residues. No other methyls were detected in NMR spectra indicating that there was essentially no protonation at any other methyl sites and Ile δ1 isotopomers of the CH_3 variety were the only ones observed.

The sample of U-[^{15}N,^{2}H], Ileδ1-[^{13}C,^{1}H] ClpP protein was prepared by overexpression of the gene for ClpP inserted into a pET9 vector in BL21(DE3)pLysS cells using the same media composition and carbon sources as indicated above for MSG. The cells were grown at 37 °C in 1 L of M9 medium. 100 mg of 4-[^{13}C,^{1}H]-3,3-^{2}*H*-α-ketobutyrate were added to the growth medium at a cell density of 0.8 1 h prior to induction with IPTG. The cells were harvested after 10 h. ClpP was purified according to the protocol of Wang et al.[26] Pure fractions of ClpP collected after gel-filtration chromatography were exchanged into 99.9% D_2O, 50 mM potassium phosphate buffer, pH 6.8 (uncorrected), containing 0.03% NaN_3, 1 mM DTT, and 0.1 mM EDTA by multiple concentration−dilution steps. The final concentration of the tetradecameric ClpP in the NMR sample was 1 mM in monomer.

NMR Spectroscopy. NMR experiments were performed on 600 and 800 MHz Varian Inova spectrometers equipped with pulsed-field gradient triple resonance probes. HMQC and HSQC methyl correlation experiments were acquired on a sample of U-[^{15}N,^{2}H], Ileδ1-[^{13}C,^{1}H] MSG at 800 MHz using the pulse schemes shown in Figure 1 at 37(5) °C and were comprised of [228(100), 768] complex points in the (^{13}C, ^{1}H) dimensions with corresponding acquisition times of [142(62) ms, 64 ms]. A relaxation delay of 1.5 s was used along with 16(32) scans/FID, giving rise to a net acquisition time of 202(173) min. The HMQC and HSQC experiments were also recorded on the sample of ClpP at 5 °C and were comprised of [40, 768] complex points in the (^{13}C, ^{1}H) dimensions with corresponding acquisition times of [20 ms, 64 ms]. A relaxation delay of 1.5 s was used along with 48 scans/FID, giving rise to a net acquisition time of 102 min.

F_1-undecoupled versions of HMQC (the double quantum pulse scheme of Figure 1 of the Supporting Information) and HSQC (using the same pulse sequence as in Figure 1a without the 180° ^{1}H pulse

(11) Rosen, M. K.; Gardner, K. H.; Willis, R. C.; Parris, W. E.; Pawson, T.; Kay, L. E. *J. Mol. Biol.* **1996**, *263*, 627−636.
(12) Gardner, K. H.; Rosen, M. K.; Kay, L. E. *Biochemistry* **1997**, *36*, 1389−1401.
(13) Mueller, G. A.; Choy, W. Y.; Yang, D.; Forman-Kay, J. D.; Venters, R. A.; Kay, L. E. *J. Mol. Biol.* **2000**, *300*, 197−212.
(14) Kay, L. E.; Bull, T. E.; Nicholson, L. K.; Griesinger, C.; Schwalbe, H.; Bax, A.; Torchia, D. A. *J. Magn. Reson.* **1992**, *100*, 538−558.
(15) Nicholson, L. K.; Kay, L. E.; Baldisseri, D. M.; Arango, J.; Young, P. E.; Bax, A.; Torchia, D. A. *Biochemistry* **1992**, *31*, 5253−5263.
(16) Gardner, K. H.; Kay, L. E. *J. Am. Chem. Soc.* **1997**, *119*, 7599−7600.
(17) Goto, N. K.; Gardner, K. H.; Mueller, G. A.; Willis, R. C.; Kay, L. E. *J. Biomol. NMR* **1999**, *13*, 369−374.
(18) Werbelow, L. G.; Marshall, A. G. *J. Magn. Reson.* **1973**, *11*, 299−313.
(19) Werbelow, L. G.; Grant, D. M. *Adv. Magn. Reson.* **1977**, *9*, 189−299.
(20) Kay, L. E.; Bull, T. E. *J. Magn. Reson.* **1992**, *99*, 615−622.
(21) Muller, N.; Bodenhausen, G.; Ernst, R. R. *J. Magn. Reson* **1987**, *75*, 297−334.
(22) Mueller, L. *J. Am. Chem. Soc.* **1979**, *101*, 4481−4484.
(23) Bax, A.; Griffey, R. H.; Hawkings, B. L. *J. Magn. Reson.* **1983**, *55*, 301−315.
(24) Bodenhausen, G.; Rubin, D. J. *Chem. Phys. Lett.* **1980**, *69*, 185−189.
(25) Howard, B. R.; Endrizzi, J. A.; Remington, S. J. *Biochemistry* **2000**, *39*, 3156−68.
(26) Wang, J.; Harting, J. A.; Flanagan, J. M. *Cell* **1997**, *91*, 447−456.
(27) Tugarinov, V.; Muhandiram, R.; Ayed, A.; Kay, L. E. *J. Am. Chem. Soc.* **2002**, *124*, 10025−10035.

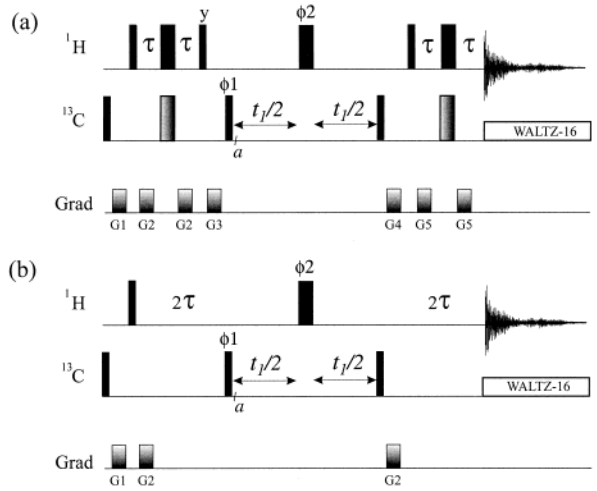

Figure 1. (a) HSQC and (b) HMQC pulse schemes used to record ^{1}H−^{13}C 2D correlations for Ile δ1 methyls. All narrow (wide) rectangular pulses are applied with flip angles of 90° (180°) along the *x*-axis unless indicated otherwise. The ^{1}H and ^{13}C carriers are positioned at 1.0 and 12 ppm, respectively. All proton pulses are applied with a field strength of 40 kHz, while ^{13}C 90° pulses are applied with a 20.5 kHz field. ^{13}C WALTZ-16 decoupling[41] during acquisition employs a 2.8 kHz field. The delay τ is set to 1.8 ms. Quadrature detection in F_1 is achieved with States-TPPI[42] of phase ϕ1 for both sequences. (a) The shaded ^{13}C 180° pulses are implemented as 400 μs Chirp adiabatic pulses[43] with an 80 kHz sweep and a maximum field strength of 12 kHz. The phase cycling employed is as follows: $\phi1 = (x, -x)$; $\phi2 = 2(x), 2(-x)$; rec = $(x, -x)$. The durations and strengths of the pulsed field gradients are as follows: g1 = (2.0 ms, 4 G/cm), g2 = (0.5 ms, 4 G/cm), g3 = (1.0 ms, 15.0 G/cm), g4 = (1.0 ms, −10 G/cm), g5 = (0.5 ms, 8 G/cm). (b) The phase cycling employed is as follows: $\phi1 = (x, -x)$; $\phi2 = 2(x), 2(y), 2(-x), 2(-y)$; rec = $(x, -x, -x, x)$. The durations and strengths of the pulsed field gradients are as follows: g1 = (1.0 ms, 15 G/cm), g2 = (0.5 ms, 20 G/cm). All gradients are applied along the *z*-axis.

during t_1 evolution) experiments were recorded on U-[^{15}N,^{2}H], Ileδ1-[^{13}C,^{1}H] MSG at 600 MHz at 37(5) °C. Data sets were comprised of [120(80), 576] complex points in the (^{13}C, ^{1}H) dimensions with corresponding acquisition times of [100(67) ms, 64 ms]. 16(32) scans/FID along with a 1.5 s relaxation delay resulted in net recording times of 105(138) minutes. Experiments were also recorded on a 100 mM ^{13}C-labeled sodium acetate sample for comparison.

All NMR spectra were processed using the NMRPipe/NMRDraw suite of programs.[28] Window functions were not employed in the indirect (^{13}C) dimensions of the HSQC and HMQC data sets for comparison of signal-to-noise ratios. The Ile δ1 methyls of MSG at 37 °C were assigned using NMR experiments to be published elsewhere. Assignments for selected Ile residues at 5 °C were possible by comparison with spectra recorded at 37 °C.

To estimate the rotational correlation time of MSG at 5 °C (in D_2O), we recorded a series of translational diffusion experiments at both 37 and 5 °C using a 2D ^{13}C,^{1}H correlation experiment that is very similar to a pulse scheme described in detail previously.[29] The ratio of diffusion constants at 37 and 5 °C can be directly related to the ratio of sample viscosities, η^{37}/η^5, at the two temperatures using the Stokes−Einstein equation ($\eta^{37}/\eta^5 = 0.38$), assuming that the structure of MSG is invariant with temperature. Previous studies have shown that the viscosity changes obtained from measurements of translational diffusion constants of DNA molecules at different temperatures could account for the changes in rotational correlation times measured.[30,31] This suggests that the ratio of viscosities measured at 37 and 5 °C can be used to obtain an estimate of the rotational correlation time, τ_C, at 5 °C, if τ_C at 37 °C is known. A value of $\tau_C = 37$ ns has been obtained for MSG in H_2O at 37 °C based on ^{15}N relaxation studies,[27] corresponding to $\tau_C = 45$ ns for the protein dissolved in D_2O (the ratio of viscosities of D_2O and H_2O at 37 °C is ∼1.21[32]). Using $\eta^{37}/\eta^5 = 0.38$, a value of $\tau_C = 118$ ns is estimated for MSG dissolved in D_2O at 5 °C. This estimate is approximately 9% larger than that predicted from the temperature dependence of the viscosity of pure D_2O[32] and similar to correlation times obtained independently from the ratios of transverse relaxation rates at 37 and 5 °C for selected isoleucine δ1 methyls. Finally, the correlation time of ClpP at 5 °C is estimated (very roughly) to be on the order of 400−450 ns based on the τ_C value determined for MSG at 5 °C and the relative molecular weights of the two proteins.

Results and Discussion

Theoretical Considerations. Figure 1 shows (a) HSQC- and (b) HMQC-based pulse sequences that can be used to record ^{1}H−^{13}C correlation spectra of macromolecules. A perusal of the literature shows that correlation spectra are most frequently obtained using HSQC schemes, likely due to the fact that improvements in ^{1}HN−^{15}N HSQC-based correlation maps over their HMQC counterparts are well documented[33,34] (at least for protonated samples) and because constant time ^{1}H−^{13}C HSQC maps are routinely recorded on uniformly ^{13}C-labeled proteins.[35,36] In what follows below, however, we will show that HMQC experiments can be superior for recording spectra of methyl groups in highly deuterated macromolecules, such as those considered here.

Consider first a description of the HSQC experiment of Figure 1a, focusing on applications to $^{13}CH_3$ groups and initially ignoring relaxation. At point "*a*" in the sequence, the magnetization of interest is given by the operator $2C_YI_Z$, where C_Y and I_Z are the Y- and Z-components of ^{13}C and ^{1}H magnetization, respectively. If the ^{1}H refocusing pulse in the center of the t_1 evolution period is neglected for the moment, then the signal evolves due to the one bond ^{1}H−^{13}C scalar coupling (coupling constant of *J*) so that the resultant 2D time-domain signal is modulated according to the relation $\cos^3 \pi J t_1 - 2 \sin^2 \pi J t_1 \cos \pi J t_1$. Fourier transformation of the t_1 time domain signal produces, therefore, a quartet structure centered at the methyl carbon chemical shift with each of the lines (denoted in what follows by L1-L4) separated by *J* Hz and with intensities in the ratio 3(L4):1(L3):1(L2):3(L1). The effect of the refocusing pulse at $t_1/2$ can be appreciated by noting that it interchanges L4 with L1 and L3 with L2 so that scalar coupled evolution is refocused at the end of the t_1 interval. Thus, in the refocused experiment of Figure 1a, the resultant signal is derived from the four components L1−L4 which all resonate at the same effective ^{13}C frequency (i.e., are superimposed in F_1).

An energy level diagram for an AX_3 spin system is shown in Figure 2, illustrating the single quantum transitions (both ^{1}H and ^{13}C) in a methyl group. The ^{13}C transitions are those that connect wave functions with horizontal lines, while the ^{1}H

(28) Delaglio, F.; Grzesiek, S.; Vuister, G. W.; Zhu, G.; Pfeifer, J.; Bax, A. *J. Biomol. NMR* **1995**, *6*, 277−293.
(29) Choy, W. Y.; Mulder, F. A. A.; Crowhurst, K. A.; Muhandiram, D. R.; Millet, I. S.; Doniach, S.; Forman-Kay, J. D.; Kay, L. E. *J. Mol. Biol.* **2002**, *316*, 101−112.
(30) Fernandes, M. X.; Ortega, A.; Lopez Martinez, M. C.; Garcia de la Torre, J. *Nucleic Acids Res.* **2002**, *30*, 1782−1788.
(31) Eimer, W.; Pecora, R. *J. Chem. Phys.* **1991**, *94*, 2324−2329.
(32) Cho, C. H.; Urquidi, J.; Singh, S.; Robinson, G. W. *J. Phys. Chem. B* **1999**, *103*, 1991−1994.
(33) Bax, A.; Ikura, M.; Kay, L. E.; Torchia, D. A.; Tschudin, R. *J. Magn. Reson.* **1990**, *86*, 304−318.
(34) Norwood, T. J.; Boyd, J.; Heritage, J. E.; Soffe, N.; Campbell, I. D. *J. Magn. Reson.* **1990**, *87*, 488−501.
(35) Vuister, G. W.; Bax, A. *J. Magn. Reson.* **1992**, *98*, 428−435.
(36) Santoro, J.; King, G. C. *J. Magn. Reson.* **1992**, *97*, 202−207.

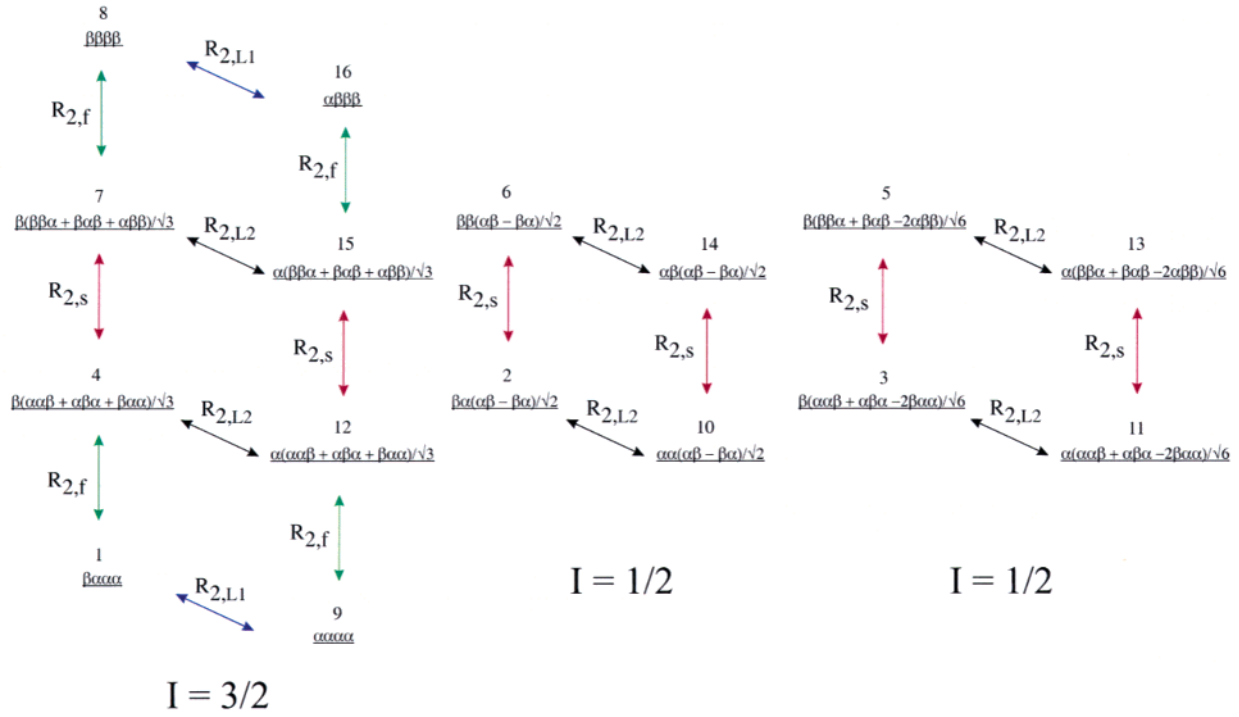

Figure 2. Energy level diagram of an isolated AX_3 (CH_3) spin system with the wave functions written in an irreducible basis representation. In this representation, the wave functions can be grouped into three manifolds (a $^3/_2$ and two $^1/_2$ manifolds) and the total spin angular momentum (I) associated with each manifold is indicated. Each of the eigenstates is numbered from 1 to 16. The first spin state in each wave function corresponds to the ^{13}C spin state, and the remaining three are associated with the proton spins. Black and blue arrows indicate transitions between ^{13}C spin states; the corresponding transverse relaxation rates of each of the transitions (in the macromolecular limit and considering only dipolar interactions; see text) are indicated at the top of each of the arrows (blue and black arrows correspond to fast-($R_{2,L1}$)- and slow-($R_{2,L2}$)-relaxing components, respectively). Green arrows indicate fast-relaxing ($R_{2,f}$) proton spin transitions, and red arrows indicate the slow-relaxing ($R_{2,s}$) proton spin transitions (see text).

transitions are those denoted by vertical lines. For example, in the case of the quartet described above, L4 derives from the transition connecting wave functions 8 and 16 ($|8><16|$), L3 (L2) is composed of $|7><15| + |6><14| + |5><13|$ ($|4><12| + |2><10| + |3><11|$), while L1 derives from the 1,9 transition. Also included in Figure 2 are the relaxation rates of the individual transitions that result from intra-methyl dipolar interactions. It is assumed that the methyl group is attached to a macromolecule (see below).

A number of studies have appeared that analyze the contributions from dipolar interactions to transverse relaxation (both ^1H and ^{13}C) in isolated methyl groups, including the effects of both autocorrelated and cross-correlated relaxation.[18,20] In the general case, a complex set of coupled relaxation equations is obtained and the (nonexponential) relaxation behavior of many of the transitions can be quite different. In the macromolecular limit ($\omega_C\tau_C \gg 1$, where τ_C is the molecular tumbling time and ω_C is the ^{13}C Larmor frequency), only spectral density terms evaluated at zero frequency are important. Considering only intra-methyl dipolar contributions to relaxation and assuming (i) $\omega_C\tau_C \gg 1$, (ii) that the methyl 3-fold rotation is very fast so that autocorrelation and cross-correlation spectral densities evaluated at zero frequency are equal,[37] and (iii) standard tetrahedral geometry, each of the transitions illustrated in Figure 2 relaxes with a single exponential.[37,38] Focusing initially on the ^{13}C transitions, we find the transverse relaxation rates of L1 ($R_{2,L1}$) and L4 ($R_{2,L4}$) are given by[37]

$$R_{2,L1} = R_{2,L4} = \left(\frac{1}{5}\right)\frac{S^2_{axis}\gamma_H^2\gamma_C^2\hbar^2\tau_C}{r_{HC}^6} \quad (1)$$

where S_{axis} is an order parameter describing the amplitude of motion of the methyl 3-fold axis, γ_i is the gyromagnetic ratio of spin i, and r_{HC} is the distance between methyl ^1H and ^{13}C spins. It can also be shown[37] that $R_{2,L2} = R_{2,L3} = (^1/_9)R_{2,L1}$. Relaxation from external protons couples density elements from different manifolds ($I = ^3/_2, ^1/_2, ^1/_2$ in Figure 2); the relaxation of lines L1−L4 are also coupled. However, so long as $2\pi J > (^3/_2)R_{1,ext}$, where $R_{1,ext}$ is the selective methyl ^1H $1/T_1$ relaxation rate, it can be shown that external spin contributions can be included to good approximation by adding the term $(^3/_2)R_{1,ext}$ to all of the rates $R_{2,Li}$ ($i = 1-4$).[39] In the case of highly deuterated proteins with methyl protonation confined to a single amino acid (Ile δ1, for example, see below), $R_{1,ext}$ is small (see below). Finally, we have not included ^{13}C CSA in the above calculations, although it would be easy to do so, since contributions to relaxation from this mechanism are considerably smaller than those from dipolar interactions.

Proton relaxation is equally important in any description of $^1H-^{13}C$ correlation spectroscopy of methyl groups.[14] Relaxation is neglected in most treatments of INEPT transfers involving $^{13}CH_3$ groups since transfer times are on the order of $1/(2J)$ which are thought to be small compared to operative relaxation times. However, this is certainly not the case for methyl groups in macromolecules (see below). The proton spectrum of a $^{13}CH_3$ group is comprised of 10 lines (see Figure 2), and density matrix calculations show that 50% of the signal originates from the

(37) Kay, L. E.; Torchia, D. A. *J. Magn. Reson.* **1991**, *95*, 536−547.
(38) Kay, L. E.; Prestegard, J. H. *J. Am. Chem. Soc.* **1987**, *109*, 3829−3835.

transitions |7><8|,|15><16| and |1><4|,|9><12| (green in Figure 2), while the remaining half of the signal is derived from the additional six transitions (red in Figure 2). Werbelow and Marshall[18] and subsequently Kay and Prestegard[38] showed that lines |7><8|,|15><16| and |1><4|,|9><12| relax very rapidly with average rates given by

$$R_{2,f} = \left(\frac{9}{20}\right)\frac{S^2_{\rm axis}\gamma_{\rm H}^4\hbar^2\tau_{\rm C}}{r_{\rm HH}^6} + \left(\frac{1}{45}\right)\frac{S^2_{\rm axis}\gamma_{\rm H}^2\gamma_{\rm C}^2\hbar^2\tau_{\rm C}}{r_{\rm HC}^6} + R_{2,\rm ext} \qquad (2.1)$$

with the first and second terms arising from intra-methyl ^{1}H−^{1}H and ^{1}H−^{13}C dipolar interactions, respectively, while the third term accounts for contributions from external spins. For a protein with $\tau_{\rm C} = 40$ ns and an assumed value of $S^2_{\rm axis} = 0.5$, the $R_{2,f}$ rate is approximately 190 s^{-1}, and the decay of these transitions must clearly be accounted for in any description of the pulse schemes of Figure 1. It can also be shown that, in the macromolecular limit and for fast methyl rotation, the decay of the remaining lines is independent of ^{1}H−^{1}H intra-methyl dipolar interactions and occurs with a rate given by[14,21]

$$R_{2,s} = \left(\frac{1}{45}\right)\frac{S^2_{\rm axis}\gamma_{\rm H}^2\gamma_{\rm C}^2\hbar^2\tau_{\rm C}}{r_{\rm HC}^6} + R_{2,\rm ext} \qquad (2.2)$$

The absence of contributions from intra-methyl proton dipolar interactions to the relaxation of 50% of the ^{1}H signal is an example of where autocorrelated and cross-correlated ^{1}H−^{1}H dipolar terms cancel in an analogous manner to the cancellation that accompanies the interference of dipolar−CSA relaxation interactions in ^{1}H−^{15}N TROSY applications.[6] In the present case, however, the effect is field independent and occurs de facto so long as the macromolecular tumbling limit applies.

A complete treatment of relaxation during the pulse scheme of Figure 1a can be accomplished by considering the trajectory of each of the density elements throughout the course of the sequence. It can be shown that the signal that is detected is given by

$$\begin{aligned}
S(t_1,t_2) = {} & [(^9/_4)\exp(-2\tau R_{2,f}) + (^9/_4)\exp(-2\tau R_{2,s})] \times \\
& \exp(-2\tau R_{2,f})\exp(-t_1 R_{2,\rm L1})\exp(-t_2 R_{2,f}) \\
& + [(^9/_4)\exp(-2\tau R_{2,f}) - (^3/_4)\exp(-2\tau R_{2,s})] \times \\
& \exp(-2\tau R_{2,f})\exp(-t_1 R_{2,\rm L2})\exp(-t_2 R_{2,f}) \\
& + [(^9/_4)\exp(-2\tau R_{2,f}) + (^9/_4)\exp(-2\tau R_{2,s})] \times \\
& \exp(-2\tau R_{2,s})\exp(-t_1 R_{2,\rm L1})\exp(-t_2 R_{2,s}) \\
& + [-(^3/_4)\exp(-2\tau R_{2,f}) + (^9/_4)\exp(-2\tau R_{2,s})] \times \\
& \exp(-2\tau R_{2,s})\exp(-t_1 R_{2,\rm L2})\exp(-t_2 R_{2,s}) \qquad (3)
\end{aligned}$$

where chemical shift evolution has been neglected (i.e., the line is on resonance in both ^{1}H and ^{13}C dimensions). Assuming that the acquisition times in each of t_1 and t_2 are long compared to the operative relaxation times, Fourier transformation of $S(t_1,t_2)$ produces a singlet with intensity at maximum height proportional to the sum of the terms given in eq 3 above with $\exp(-t_1 R_{2,\rm L1})$, $\exp(-t_1 R_{2,\rm L2})$, $\exp(-t_2 R_{2,f})$, and $\exp(-t_2 R_{2,s})$ replaced by $T_{2,\rm L1}$, $T_{2,\rm L2}$, $T_{2,f}$, and $T_{2,s}$ respectively, where $T_{2,i} = 1/R_{2,i}$.

A number of limiting cases of eq 3 are worth discussing. First, in the absence of relaxation magnetization that evolves in the outer carbon lines (L1,L4) during t_1 contributes $^3/_4$ of the net signal. (As an interesting aside, in ^{13}C direct observe spectroscopy, only 25% of the signal derives from the outer components.) The situation changes quite dramatically in the presence of relaxation, however. Since the outer ^{13}C lines relax 9-fold faster than the inner lines[37] (neglecting contributions from external protons), they contribute very little to the intensity of signal in applications involving very high molecular weight proteins (less than 20% for $\tau_{\rm C} = 40$ ns, $S^2_{\rm axis} = 0.5$). As a further example of how relaxation during the delays in the sequence can affect the intensity of the resultant signal, consider a deuterated protein in which Ile residues are protonated at the C$^{\delta 1}$ position. The correlation time of the protein, $\tau_{\rm C}$, and the square of the methyl axis order parameter, $S^2_{\rm axis}$, are set to 40 ns and 0.5, respectively. Values of $R_{2,\rm L1} \approx 67$ s^{-1}, $R_{2,\rm L2} \approx 7.5$ s^{-1}, $R_{2,f} \approx 186$ s^{-1}, and $R_{2,s} \approx 16$ s^{-1} are calculated from the relaxation expressions above, including the effects of external protons (<1 s^{-1} to $R_{2f,s}$) and deuterons (≈ 8 s^{-1} to $R_{2f,s}$) using average distances obtained from the X-ray structure of MSG[25] and assuming an order parameter of 1 for the methyl-external spin interactions. In this case, the net signal immediately prior to detection, $S(t_1 = 0,t_2 = 0)$, is 52% of what it would be in the absence of relaxation. For a protein with $\tau_{\rm C} = 150$ ns, $S^2_{\rm axis} = 0.5$, this number decreases to less than 25%.

The steps in the derivation leading to eq 3 make clear that the number of ^{1}H 90° pulses in the HSQC sequence is particularly damaging to the sensitivity of the experiment. The first 90° pulse creates ^{1}H magnetization with 50% of the signal relaxing very rapidly (see above) with a rate of $R_{2,f}$ and 50% much more slowly with a rate of $R_{2,s}$. Subsequent ^{1}H 90° pulses interconvert fast- and slow-relaxing components, significantly reducing the fraction of the magnetization that relaxes slowly for the complete sequence. Thus, for very large molecules, only signal that is derived from the last term in eq 3, $\{(9/4)\exp(-4\tau R_{2,s})\ T_{2,L2}T_{2,s}\}$, and which relaxes with the largest time constants throughout the sequence, contributes appreciably to the intensity of the recorded correlations. It is clearly of interest, therefore, to consider other pulse schemes where the effects of relaxation are very much less detrimental to sensitivity.

Figure 1b illustrates the HMQC sequence used to record ^{1}H−^{13}C correlation maps. As with the description of the HSQC scheme above, we initially neglect relaxation and assume that both ^{13}C and ^{1}H methyl spins are on resonance. The magnetization of interest at point "*a*" is given, therefore, by $2C_{\rm Y}I_{\rm X}$, corresponding to a linear superposition of double and zero-quantum coherences. In the absence of the ^{1}H 180° pulse in the center of the t_1 period evolution of the signal due to the ^{1}H−^{13}C one-bond scalar coupling during t_1 results in its modulation by the factor $\cos^2 \pi J t_1$; subsequent Fourier transformation of the signal gives rise to a multiplet structure comprised of three lines (L1′,L2′,L3′), each separated by J Hz, corresponding to a 1(L1′):2(L2′):1(L3′) triplet. Application of the ^{1}H 180° pulse at $t_1/2$ interconverts L1′ and L3′ so that the multiplet structure collapses into a singlet (superposition of L1′,L2′,L3′). Recalling that the ^{13}C spectrum of a methylene

(39) Kay, L. E.; Nicholson, L. K.; Delaglio, F.; Bax, A.; Torchia, D. A. *J. Magn. Reson.* **1992**, *97*, 359−375.

group is a 1:2:1 triplet (in the absence of relaxation), it becomes clear that from the perspective of ^{13}C evolution, and as we show below also relaxation, the creation of $2C_YI_X$ effectively carries out a "spectroscopic" conversion of a methyl into a methylene. A more elaborate calculation which considers all of the proton transitions in a methyl group (Figure 2) shows that $2C_YI_X = 2C_YI_{X,1} + 2C_YI_{X,2} + 2C_YI_{X,3}$ with $2C_YI_{X,i} = 2C_YI_{X,i}\{|\beta\beta><\beta\beta| + |\alpha\beta><\alpha\beta| + |\beta\alpha><\beta\alpha| + |\alpha\alpha><\alpha\alpha|\}$ where $\{\alpha,\beta\}$ are spin states of methyl protons $j,k \neq i$. The first and last terms in the above expression give rise to L3′ and L1′, while the middle two terms contribute to L2′, thus establishing the relation between single quantum ^{13}C magnetization in a CH_2 group and $^1H-^{13}C$ double-zero quantum in a CH_3 moiety.

Prestegard and Grant[40] have derived expressions for the contribution from dipolar interactions to the transverse relaxation rates of the ^{13}C multiplet components of an AX_2 spin system ($A = {}^{13}C$, $X = {}^1H,{}^{19}F$). In the case that the methylene rotates rapidly about an averaging axis (each AX bond vector makes the same angle with respect to this axis), which in turn tumbles in the macromolecular limit, the central carbon line of the triplet is free of any relaxation resulting from intra-methylene dipole−dipole interactions. In a similar manner, it can be shown that there are no intra-methyl dipole−dipole contributions to the relaxation of L2′. A calculation shows that, in the macromolecular limit and for very rapid methyl rotation, the average relaxation rates of L1′−L3′ in the sequence of Figure 1b are given by

$$R_{2,L1'} = R_{2,L3'} = \left(\frac{4}{45}\right)\frac{S^2_{axis}\gamma_H^2\gamma_C^2\hbar^2\tau_C}{r_{HC}^6} + \left(\frac{9}{20}\right)\frac{S^2_{axis}\gamma_H^4\hbar^2\tau_C}{r_{HH}^6}$$

$$R_{2,L2'} = 0 \qquad (4)$$

where only intra-methyl dipolar contributions are included. The first and second terms in the expression for $R_{2,L1'} = R_{2,L3'}$ derive from $^1H-^{13}C$ and $^1H-^1H$ dipolar interactions (both autocorrelation and cross-correlation), respectively. Remarkably, autocorrelation and cross-correlation dipolar contributions completely cancel for L2′ and, this cancellation is independent of field, a completely optimized TROSY effect that results from the combination of rapid methyl rotation and very slow overall molecular tumbling. External contributions to the relaxation rates can be included by adding $R_{1,ext} + R_{2,ext}$ to the terms above, where $R_{1,ext}$ (selective spin flip rate of a methyl proton, neglecting cross-correlated relaxation involving external protons) derives from the interconversion of $2C_YI_{Xi}$, $4C_XI_{Xi}I_{Zj}$, and $8C_YI_{Xi}I_{Zj}I_{Zk}$ during the t_1 evolution time and concomitant ^1H spin flips involving external protons. $R_{2,ext}$ includes contributions to transverse relaxation from external protons and deuterons. For a U-[$^{15}N,^2H$], Ileδ1-[$^{13}C,^1H$] protein tumbling isotropically with $\tau_C = 40$ ns and $S^2_{axis} = 0.5$, $R_{2,L1'} = R_{2,L3'} \approx 200\ s^{-1}$, while $R_{2,L2'} \approx 8\ s^{-1}$. The nonzero value of $R_{2,L2'}$ reflects the fact that contributions from external protons and deuterons have been included, using average distances from the X-ray structure of glyoxylate-bound MSG[25] and assuming an order parameter of 1 for the methyl-external spin interactions. It is clear that lines L1′ and L3′ will make negligible contributions to methyl correlations in HMQC spectra.

Including the effects of relaxation during the complete pulse scheme, the signal intensity (neglecting chemical shift evolution) is given by

$$S(t_1,t_2) = 6\exp(-4\tau R_{2,f})\exp(-t_1R_{2,L1'})\exp(-t_2R_{2,f}) + 6\exp(-4\tau R_{2,s})\exp(-t_1R_{2,L2'})\exp(-t_2R_{2,s}) \quad (5.1)$$

Fourier transformation of $S(t_1,t_2)$ gives rise to a signal with maximum intensity proportional to

$$6\exp(-4\tau R_{2,f})T_{2,L1'}T_{2,f} + 6\exp(-4\tau R_{2,s})T_{2,L2'}T_{2,s} \quad (5.2)$$

The major strength of the HMQC sequence for applications involving high molecular weight proteins is that throughout the experiment there is no mixing between fast and slowly relaxing components, excluding the effects of spin flips with external protons which can be minimized through the construction of highly deuterated proteins. In this regard, the application of only a single 90° ^1H pulse is critical. In the limit that $\tau \gg 1/R_{2,f}$, the last term in each of eqs 3 and 5 dominates, and a comparison of calculated intensities in HMQC and HSQC correlation maps gives $I_{HMQC}/I_{HSQC} \approx 2.7T_{2,L2'}/T_{2,L2}$. At first glance, it might appear that $T_{2,L2'} \gg T_{2,L2}$, since $T_{2,L2'}$ does not include contributions from intra-methyl dipolar interactions, while $T_{2,L2}$ does. However, $T_{2,L2'}$ is more sensitive to external relaxation contributions than $T_{2,L2}$ (see above). In the case of a U-[$^{15}N,^2H$], Ileδ1-[$^{13}C,^1H$] protein, for example, calculations using the structure of MSG and experiments performed on a U-[$^{15}N,^2H$], Ileδ1-[$^{13}C,^1H$] MSG sample in D_2O show that $T_{2,L2'} \approx T_{2,L2}$. The above arguments predict, therefore, that for samples with a low proton density significant sensitivity gains in HMQC spectra should be obtained relative to their HSQC counterparts (approximately 2.5-fold), and in the subsequent section, we show that this is indeed the case.

Experimental Verification. An important consideration in ensuring optimal sensitivity of methyl correlations in HSQC/HMQC experiments is to minimize the contributions to relaxation of the methyl spins from external sources. This is particularly the case for the HMQC scheme, where the contributions to $R_{2,L2'}$ from intra-methyl dipolar interactions are zero, but where line L2′ is vulnerable to decay from interactions with external protons since it derives from a coherence that is proportional to $I_{TR}C_{TR}$, where the subscript TR denotes transverse magnetization. For this reason, we have produced a highly deuterated sample of MSG dissolved in D_2O with protonation only at the $C^{\delta1}$ positions of Ile groups. In this way, external protons for a given Ile derive only from other Ile residues. Proteins with this labeling pattern can be easily expressed using a highly deuterated medium (D_2O, deuterated glucose) supplemented by 4-[$^{13}C,^1H$]-3,3-$^2H_2$-α-ketobutyrate, as described by Goto et al.[17] (see Materials and Methods).

In the previous section, a discussion of the differential relaxation of the lines which contribute to $^1H-^{13}C$ methyl correlations in HSQC and HMQC spectra was presented. As described above, a consequence of these differences in relaxation rates is that certain lines contribute much less to $^1H-^{13}C$

(40) Prestegard, J. H.; Grant, D. M. *J. Am. Chem. Soc.* **1978**, *100*, 4664−4668.
(41) Shaka, A. J.; Keeler, J.; Frenkiel, T.; Freeman, R. *J. Magn. Reson.* **1983**, *52*, 335−338.
(42) Marion, D.; Ikura, M.; Tschudin, R.; Bax, A. *J. Magn. Reson.* **1989**, *85*, 393−399.
(43) Kupce, E.; Freeman, R. *J. Magn. Reson., Ser. A.* **1995**, *115*, 273−276.
(44) Brünger, A. T.; Adams, P. D.; Clore, G. M.; DeLano, W. L.; Gros, P.; Grosse-Kunstleve, R. W.; Jiang, J.; Kuszewski, J.; Nilges, M.; Pannu, N. S.; Read, R. J.; Rice, L. M.; Simonson, T.; Warren, G. L. *Acta Crystallogr.* **1998**, *D54*, 905−921.

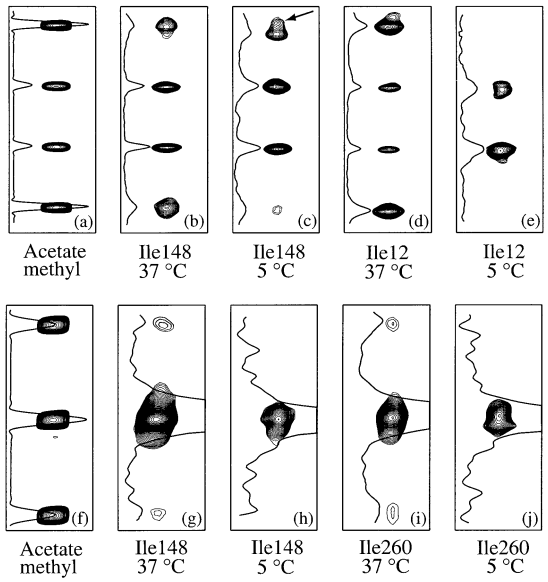

Figure 3. ^{13}C-multiplet structures of selected Ile δ1 peaks of MSG and the methyl group of sodium acetate from ^{1}H-coupled HSQC (a−e, upper row) and HMQC (f−j, lower row) spectra. 1D traces taken at each peak position are shown. "Quartets" of (a) the methyl of sodium acetate (approximate intensity ratio in the quartet 4:1:1:4), (b) Ile148 at 37 °C, (c) Ile148 at 5 °C (the outer fast-relaxing lines are still visible but are significantly reduced in intensity compared to 37 °C; the arrow indicates the position of the outer peak, partially overlapped with a peak from another HSQC multiplet), (d) Ile12 at 37 °C, and (e) Ile12 at 5 °C (only the two slowly relaxing inner lines are detected). "Triplets" of (f) the methyl of sodium acetate (approximate intensity ratios of 1:1.8:1), (g) Ile148 at 37 °C, (h) Ile148 at 5 °C (only the central line, L2′, is visible), (i) Ile260 at 37 °C, and (j) Ile260 at 5 °C (only L2′ is visible). Since the intensities of the outer lines of the HMQC mutiplets (L1′, L3′) are extremely small relative to the inner line, L2′ (<3.5% at 37 °C and only observed for Ile 148 260), the HMQC spectra are drawn at ∼10-fold lower contour levels than their HSQC counterparts.

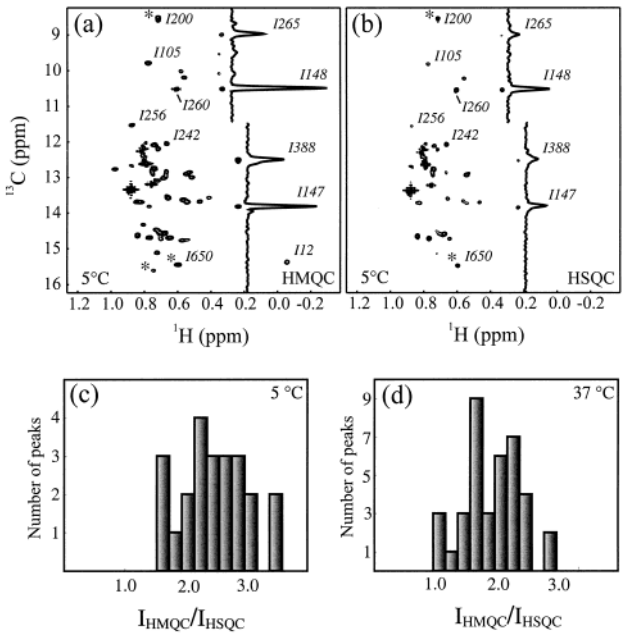

Figure 4. Resolution-enhanced 800 MHz ^{1}H−^{13}C HMQC (a) and HSQC (b) spectra of U-[^{15}N,^{2}H], Ileδ1-[^{13}C,^{1}H] MSG (82 kDa) recorded at 5 °C ($\tau_C \approx 118$ ns) with net measuring times of 173 min. The spectra were obtained with identical acquisition parameters, and a 60°-shifted squared cosine window function was employed in both dimensions. Selected Ile δ1 methyls are labeled with residue numbers. Peaks marked with asterisks are folded in the ^{13}C dimension. The spectra are plotted at the same contour levels, and the 1D traces at the positions of selected peaks are shown to facilitate comparison. Histograms of signal-to-noise ratios of correlations from HMQC and HSQC spectra (I_{HMQC}/I_{HSQC}) recorded at (c) 5 °C for 23 peaks whose intensities could be quantified in both data sets (average $I_{HMQC}/I_{HSQC} = 2.6$) and (d) 37 °C for 38 peaks (average $I_{HMQC}/I_{HSQC} = 1.9$).

correlations in HSQC or HMQC maps than others, with the relative contribution very much dependent on the molecular correlation time. This is illustrated in Figure 3, where ^{1}H−^{13}C HSQC (a−e) and HMQC (f−j) correlations are plotted. The HSQC correlations have been recorded using the pulse scheme of Figure 1a with the ^{1}H 180° refocusing pulse at $t_1/2$ removed, so that lines L1−L4 can be observed individually. If the four lines were to relax with the same decay constant, a 3:1:1:3 quartet structure would be expected, and deviations from this ratio are anticipated in the presence of differential relaxation. The spectrum recorded on acetate is shown in Figure 3a, and of interest, a 4:1:1:4 multiplet is obtained, suggesting that differential relaxation effects are not unimportant in this small molecule as well. Nevertheless, it is certainly the case that the outer lines are significantly more intense than the inner ones, as expected. In panels b−e, multiplet components are shown for Ile residues obtained in an HSQC spectrum recorded on a sample of U-[^{15}N,^{2}H], Ileδ1-[^{13}C,^{1}H] MSG dissolved in D_2O. Panels b,c [d,e] show multiplet components for Ile 148 [12] at 37 °C ($\tau_C = 45$ ns) and at 5 °C ($\tau_C = 118$ ns). For Ile 148 at 37 °C, the multiplet structure is very different from that obtained with acetate, with much of the intensity associated with the inner lines. The relative size of the outer lines decreases yet further with temperature (compare c with b and e with d). The decrease in the intensity of the outer components as a function of correlation time is quite apparent for Ile 12 where they are quite large at 37 °C yet completely absent at 5 °C. Since all lines, L1−L4, ultimately give rise to the observed signal in the case of a completely decoupled spectrum, it is clear that in applications to high molecular weight systems the contributions from the outer lines can be quite small.

To illustrate how L1′−L3′ contribute to methyl correlations in HMQC spectra, we have recorded a double-quantum correlation map where the ^{1}H−^{13}C scalar coupling is allowed to evolve during t_1. Note that this spectrum cannot be obtained by simply removing the ^{1}H 180° pulse from the scheme of Figure 1b since ^{1}H chemical shift would subsequently not be refocused. We have therefore used an enhanced sensitivity ^{1}H−^{13}C double quantum scheme, illustrated in the Supporting Information. Figure 3f shows the correlation map obtained for acetate, where a 1:1.8:1 triplet is observed (a 1:2:1 triplet is expected in the absence of relaxation). Spectra recorded at 37 °C on a U-[^{15}N,^{2}H], Ileδ1-[^{13}C,^{1}H] MSG sample in D_2O establish that the outer lines are nearly gone (Ile 148 and 260 in panels g and i), while at 5 °C they have completely disappeared. Note that the outer lines in the double-quantum correlation map are much smaller than the corresponding components in the HSQC data set, due to their significantly higher relaxation rates.

Figure 4a,b compare ^{1}H−^{13}C methyl correlation maps recorded on U-[^{15}N,^{2}H], Ileδ1-[^{13}C,^{1}H] MSG in D_2O at 5 °C, 800 MHz using HMQC (a) and HSQC (b) pulse schemes. For comparison, both spectra are plotted at the same level, and it is quite clear that the HMQC data set has significantly higher sensitivity. This is also illustrated in the pair of traces selected at 0.23 and 0.34 ppm in the ^{1}H dimension. Figure 4c shows a histogram of the ratios of signal-to-noise in HMQC and HSQC

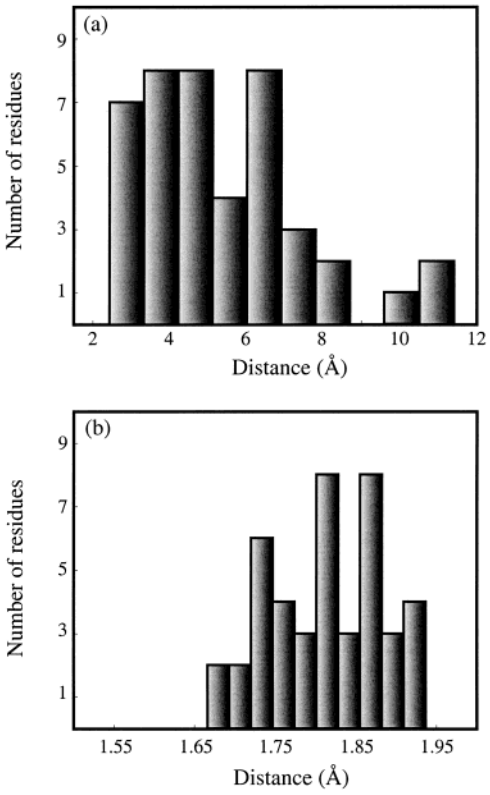

Figure 5. Histograms of (a) $<r^k_{\mathrm{eff,H}}>$ and (b) $<r^k_{\mathrm{eff,D}}>$ in U-[^{15}N,^{2}H], Ileδ1-[^{13}C,^{1}H] MSG in D_2O (see text). Distances were calculated from the X-ray coordinates of glyoxylate bound MSG (Protein Data Bank accession code 1d8c)[25] with protons added to the X-ray structure using the program CNS.[44]

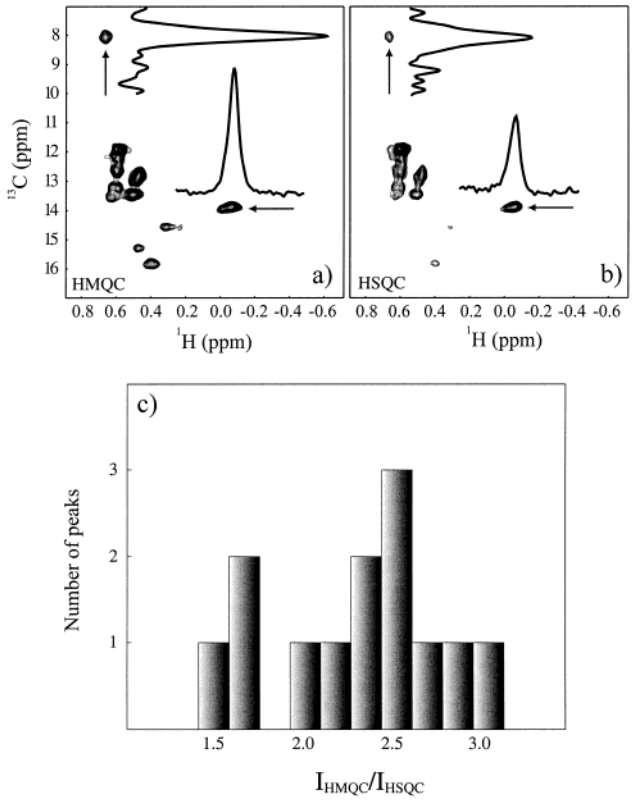

Figure 6. Resolution-enhanced 800 MHz ^{1}H$-^{13}$C spectra of U-[^{15}N,^{2}H], Ileδ1-[^{13}C,^{1}H] tetradecameric ClpP (305 kDa, 193 residues per monomer) at 5 °C. Both spectra were recorded with identical sets of parameters (net acquisition times of 102 min) and are plotted at the same contour levels. 1D traces from the peak positions indicated with arrows are shown. (c) Histogram of signal-to-noise ratios of correlations in the HMQC and HSQC spectra ($I_{\mathrm{HMQC}}/I_{\mathrm{HSQC}}$) for 12 peaks (out of 16 Ile residues per monomeric unit) whose intensities could be quantified in both HMQC and HSQC data sets (average $I_{\mathrm{HMQC}}/I_{\mathrm{HSQC}} = 1.9$).

spectra recorded at 5 °C ($I_{\mathrm{HMQC}}/I_{\mathrm{HSQC}}$), and on average, a gain in signal of a factor of 2.6 is noted in the HMQC data set. The relative sensitivity gains in HMQC versus HSQC maps of MSG recorded at 37 °C have also been compared, and not unexpectedly, $I_{\mathrm{HMQC}}/I_{\mathrm{HSQC}}$ decreases as the correlation time is reduced, although on average a gain of a factor of 1.9 is obtained, Figure 4d. Of interest, we have also recorded constant time (CT)-HMQC and HSQC data sets (constant time delay set to 28 ms) on the U-[^{15}N,^{2}H], Ileδ1-[^{13}C,^{1}H] MSG sample; although CT spectroscopy is not recommended in the present case, since ^{13}C labeling is confined to Ile methyls, we wanted to establish that the sensitivity gains obtained using the schemes of Figure 1 could also be realized in the event that a fully ^{13}C-labeled sample was studied. Average $I_{\mathrm{CT-HMQC}}/I_{\mathrm{CT-HSQC}}$ ratios of 2.1 and 2.9 were obtained for spectra recorded at 37 and 5 °C, respectively.

The average effective sum of distances between a methyl proton of a given Ile residue, say k, and all other Ile protons, $<r^k_{eff,H}>$, can be calculated according to

$$\frac{1}{3}\sum_{i=1}^{3}\left(\sum_{j}\left(\frac{1}{r_{ij}^{6}}\right)\right)^{-1/6}$$

where r_{ij} is the distance between proton i of methyl k and proton j of another Ile. Figure 5a illustrates such a distribution of distances obtained for the 44 Ile residues of MSG, calculated from the X-ray structure of the glyoxylate bound form of the protein.[25] The average value of $<r^k_{\mathrm{eff,H}}>$ is 5.5 Å, and contributions to relaxation from inter-Ile dipolar interactions are minimal (calculated to be less than 1 s^{-1} for a correlation time of 40 ns). Figure 5b illustrates the distribution of effective sums of distances between protons of a given Ile and all of the deuterons in U-[^{15}N,^{2}H], Ileδ1-[^{13}C,^{1}H] MSG. An average value of 1.8 Å is obtained, and the dipolar contribution to the relaxation of transverse proton magnetization, for example, from external deuterons is calculated to be 8 s^{-1} on average for a protein tumbling with a correlation time of 40 ns, assuming an order parameter of 1 for the methyl-external spin interactions. A reasonable correlation between peak intensities in HMQC correlation maps of U-[^{15}N,^{2}H], Ileδ1-[^{13}C,^{1}H] MSG and $<r^k_{eff,H}>$ is obtained; however, other factors, such as methyl dynamics both on fast (increased intensity) and slow (decreased intensity) time scales, can also significantly affect the strength of correlations.

It is well-known that the quality of ^{1}H$-^{15}$N TROSY correlation spectra significantly degrades as the level of protonation in samples increases,[6] and it seems clear that similar degradations will be observed in the methyl experiments described here. With this in mind, we are currently developing protocols to produce highly deuterated proteins with protonation at only one of each of the two methyls of Val and Leu residues, and the results from such a study will be reported subsequently.

As a final demonstration of the improvements in sensitivity of HMQC versus HSQC methyl correlation maps that can be obtained in cases of dilute protonated methyl groups in high molecular weight systems, we have recorded spectra of the

protease ClpP, a 14-mer where each identical subunit[26] consists of 193 amino acids (305 kDa molecular weight). The ClpP protease in *E. coli* degrades proteins that have first been unfolded and targeted for degradation by the ClpX chaperone.[26] As an initial step in studying this process, we have prepared U-[^{15}N,^{2}H], Ileδ1-[^{13}C,^{1}H]-labeled ClpP in D_2O and recorded spectra of the protein at 5 °C (subunit concentration of 1mM). Each subunit contains 16 Ile residues, and since the subunits are equivalent,[26] 16 correlations are expected in the spectra. Conservatively, we have been able to count at least 14 such correlations in the HMQC spectrum of Figure 6a, recorded in 1.5 h at a field strength of 800 MHz. As observed in studies of MSG, HMQC spectra are superior to HSQC maps, Figure 6a,b, with sensitivity gains varying between factors of 1.5 to 3.1 depending on the residue, Figure 6c. The average sensitivity gain obtained, a factor of 1.9, is slightly less than the expected value of approximately 2.5, likely the result of conformational heterogeneity which can affect HMQC spectra more than HSQC data sets. It is noteworthy in this regard that spectra recorded at temperatures greater than 5 °C showed significant line broadening.

In summary, it has been shown that significant sensitivity gains can be obtained in HMQC versus HSQC spectra of dilute protonated methyl groups in macromolecules. The sensitivity gains can be traced to the differential relaxation of the transitions that give rise to the correlations and to the way in which magnetization is transferred in each of the experiments. The observed effect results from interference between intra-methyl dipolar interactions and as such is magnetic field independent. To our knowledge, this is the first example of a TROSY enhancement resulting exclusively from dipolar interactions. The high quality of spectra recorded at 5 °C on systems ranging from 80 to 305 kDa in short measuring times suggests that studying molecular structure and dynamics with methyl probes will be feasible for many supramolecular systems.

Acknowledgment. This research was supported by a grant from the Canadian Institutes of Health Research (C.I.H.R) to L.E.K. The authors thank Professor Walid Houry, University of Toronto, for providing the construct of ClpP, and Professors Cheryl Arrowsmith, Ontario Cancer Institute, and Julie Forman-Kay, Hospital for Sick Children, for providing laboratory facilities for sample production. The authors are grateful to Professor Nikolai Skrynnikov (Purdue) for a critical evaluation of the manuscript and Professor Mike Rosen (U.T. Southwestern Medical Center) for useful discussions. V.T. is a recipient of a Human Frontiers Science Program Postdoctoral Fellowship, P.M.H. holds a C.I.H.R predoctoral fellowship, and J.E.O. is the recipient of a Natural Sciences and Engineering Research Council of Canada postgraduate scholarship. L.E.K. holds a Canada Research Chair in Biochemistry.

Supporting Information Available: One figure of a sensitivity enhanced double quantum pulse scheme for recording ^{1}H−^{13}C correlations. This material is available free of charge via the Internet at http://pubs.acs.org.

JA030153X